Electronic Supplementary Material (ESI) for Journal of Materials Chemistry A.

Supporting information

Enzyme-like MOFs: Synthetic molecular receptors with high binding capacity and their application in selective photocatalysis

Libin Wan,[a,c] Hui Liu,[a] Chuixiu Huang[b*] and Xiantao Shen[a*]

[a] *State Key Laboratory of Environment Health (Incubation), Key Laboratory of Environment and Health, Ministry of Education, Key Laboratory of Environment and Health (Wuhan), Ministry of Environmental Protection, School of Public Health, Tongji Medical College, Huazhong University of Science and Technology, #13 Hangkong Road, Wuhan, Hubei, 430030, China*

[b] *Department of Forensic Medicine, Huazhong University of Science and Technology, #13 Hangkong Road, Wuhan, Hubei 430030, China*

[c] *Henan Business Science Research Institute Co. Ltd., Henan Academy of Sciences, #87 Wenhua Road, Zhengzhou, 450002, China.*

** Corresponding author.*

E-mail address: xtshenlab@hust.edu.cn (X. Shen)
chuixiuh@hust.edu.cn (C. Huang)

1. Chemical reagents

Zirconium chloride ($ZrCl_4$, 99.5%), ferric chloride hexahydrate ($FeCl_3 \cdot 6H_2O$), 4-nitrophenol (4NP), *N*,*N*-dimethylformamide (DMF), phenol, benzoic acid and methanol were purchased from Sinopharm Chemical Reagent Co., Ltd. (Shanghai, China). Sulfadimidine (SM2, 99%), sulfamethoxazole (SMZ, 98%), sulfa benzoyl (SB, 98%), metanilic acid (MA, 98%), sulfanilamide (SA, 98%), sulfadimethoxine (SDM, 98%), ketoprofen (KET, 98%), naproxen (NAP, 98%), caffeine (CAF, 98%) and propranolol (PRO, 98%) were obtained all from Aladdin Chemical Reagent Co. (Shanghai, China). 2-Aminoterephtalic acid (NH_2-BDC, 98%) was obtained from Energy Chemical (Shanghai, China). Rhodamine B (RhB, 95%) was supplied by Sigma-Aldrich (Shanghai, China). All chemicals were obtained from commercial without further purification.

2. Instrumentations

The crystalline structures of materials were characterized by X-ray diffraction (XRD) on Empyrean XRD system with CuKα radiation. The XRD patterns were recorded in the 2θ range from 5° to 50°. FT-IR spectra of materials between 4000 cm^{-1} and 400 cm^{-1} were recorded by a VERTEX 70 spectrometer (Bruker, Germany). Surface morphologies of materials were observed by scanning electron microscopy (SEM, JSM-6710F) and transmission electron microscope (TEM, Tecnai G2T20). Brunauer-Emmett-Teller (BET) surface areas were determined by nitrogen adsorption-desorption isotherm at 77 K on MICROMETERS ASAP 2020 analyzer, and pore size distribution calculation was obtained based on Density Functional Theory (DFT) analysis. The elemental composition and the chemical state of materials were analyzed by X-ray photoelectron spectroscopy (XPS, Thermo ESCALAB 250XI). Solid state ^{1}H-NMR spectra and ^{13}C-NMR spectra of materials were measured on an Agilent 600M solid nuclear magnetic spectroscopy.

3. Analytical methods

HPLC-UV analysis: The concentrations of the substances were measured respectively by high performance liquid chromatography (HPLC). Typically, a Dionex Ultimate 3000 system (Dionex, Germering, Germany) equipped with a LPG-

3400RS pump and a VWD-3400RS UV/vis detector was used for HPLC chromatographic analysis. A Symmetry C18 column (100 × 2.1 mm, 3.5 μm) was used for chromatographic separation. Mobile phase A was 0.1% formic acid containing 5% of methanol (v/v), and mobile phase B was methanol containing 5% of 0.1% formic acid (v/v). For the determination of KET, NAP, CAF, PRO, RhB, benzoic acid and phenol, the mobile phase was 55% of B and 45% of A with a flow rate of 0.6 mL min^{-1}, the injection volume was 10 μL and the UV/vis detector was set at 272 nm. For the simultaneous detection of KET and SDM in the binary system, the mobile phase B was increased from 30% to 70% in 1 min, and held constant for additional 2 min, then decreased to 30% in 1 min, which was kept for 2 min for equilibration. For the determination of SM2, SMZ, MA, SA and SB, the mobile phase was 10% of B and 90% of A with a flow rate of 0.8 mL min^{-1}, the injection volume was 5 μL and the UV/vis detector was set at 230 nm. The concentrations of CAF and PRO were determined respectively by the UV-vis adsorption on a UV-visible spectrophotometer (Shimazu UV-1800).

LC-MS analysis: Analysis of the intermediate products during the photocatalytic degradation of SM2 were performed on a Ultimate 3000 UPLC system coupled to a TSQ Quantum Access triple quadrupole mass spectrometer (Thermo Scientific, USA) equipped with a Hypersil GOLD C18 column (100 mm × 2.1 mm, 5 μm). The injection volume and flow rate were 5 μL and 0.2 mL min^{-1}, respectively. Mobile phase A was 0.1% formic acid (containing 5 mmol L^{-1} CH_3COONH_4), and mobile phase B was acetonitrile. In 1 min, mobile phase B was increased from 10% to 60%, and kept constant for additional 5 min, then decreased to 10% in 1 min, and then kept for 3 min for equilibration. The ion source was operated in both positive and negative mode by scanning from *m/z* 40 to 300 and from *m/z* 40 to 200, respectively.

4. Synthesis of ketoprofen (KET) imprinted UiO-66_NH_2

KET imprinted MOFs (the imprinted UiO-66_NH_2) was prepared by an in-situ self-assembly strategy. In the typical procedure, 0.320 g of $ZrCl_4$ and 0.352 g KET were dissolved in 80 mL of DMF to obtain a homogenous solution. After an ultrasonication for 30 min, 0.124 g of NH_2-BDC was added into the solution. The mixture was transferred into a 100 mL of Teflon liner. The Teflon liner vessel was sealed and placed in a preheated oven at 120 °C for 48 h. After cooling to room temperature, the materials were collected by centrifuging at 10000 rpm for 10 min and washed with 30 mL of methanol twice. To remove the template and excess metal ion and organic ligand inside imprinted UiO-66_NH_2, the materials were treated with 100 mL of DMF (containing 0.4 mL of concentrated HCl) at 90 °C for 12 h under stirring. After repeating the treatment, the product was washed by 30 mL of methanol for three times, and then dried in vacuum oven at 60 °C for overnight. In this way, the imprinted UiO-66_NH_2 was obtained. The non-imprinted UiO-66_NH_2 was prepared in the same way as that for the imprinted UiO-66_NH_2 except the addition of the KET template.

5. Characterization of imprinted UiO-66_NH_2 and non-imprinted UiO-66_NH_2

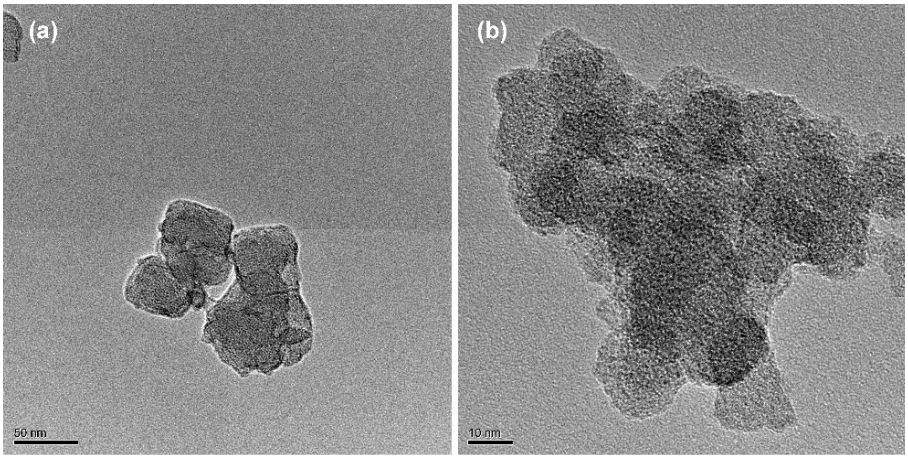

Fig. S1. TEM images of the non-imprinted UiO-66_NH_2 (a) and the imprinted UiO-66_NH_2 (b).

Table S1. The atom content of the C, N, O and Zr in the non-imprinted UiO-66_NH_2, imprinted UiO-66_NH_2 containing KET and imprinted UiO-66_NH_2.

Samples	C 1s (at. %)	N 1s (at. %)	O 1s (at. %)	Zr 3d (at. %)
Non-imprinted UiO-66_NH_2	56.9	6.3	31.3	5.5
Imprinted UiO-66_NH_2 containing KET	57.1	6.3	32.2	4.4
Imprinted UiO-66_NH_2	54.8	5.6	34.0	5.6

6. Adsorption performance of KET on the imprinted UiO-66_NH_2

The effect of pH on the adsorption performance of KET over the imprinted UiO-66_NH_2 and non-imprinted UiO-66_NH_2 was studied by adjustment of sample solution pH from 3.4 to 9.3. As shown in **Fig. S2a**, the specific binding capacity of KET on both imprinted UiO-66_NH_2 and non-imprinted UiO-66_NH_2 remained almost no change within the pH range of 3.4 to 6.8. Further increasing the sample solution pH from 6.8 to 9.3, the adsorption performance of KET on both imprinted UiO-66_NH_2 and non-imprinted UiO-66_NH_2 became dramatically inferior, while the imprinting effect of imprinted UiO-66_NH_2 was almost unaffected in the tested whole range of pH. These results indicated that the imprinted UiO-66_NH_2 exhibited good adsorption performance in a wide pH range, and the sample solution pH was fixed at 6.8 in the subsequent binding experiments.

The zeta potentials of imprinted UiO-66_NH_2 and non-imprinted UiO-66_NH_2 were also measured. The net charge versus pH for the materials was presented in **Fig. S2b**. It revealed that the isoelectric point of imprinted UiO-66_NH_2 and non-imprinted UiO-66_NH_2 were 5.26 and 4.01, respectively. The increase of the isoelectric point of imprinted UiO-66_NH_2 was due to the fact that the imprinting of KET partially replaced the ligand (NH_2-BDC) and occupied some unsaturated Zr(Ⅳ) site during the synthesis. The removal of KET not only provided additional defect spaces, but also exposed more Zr(Ⅳ) active sites.

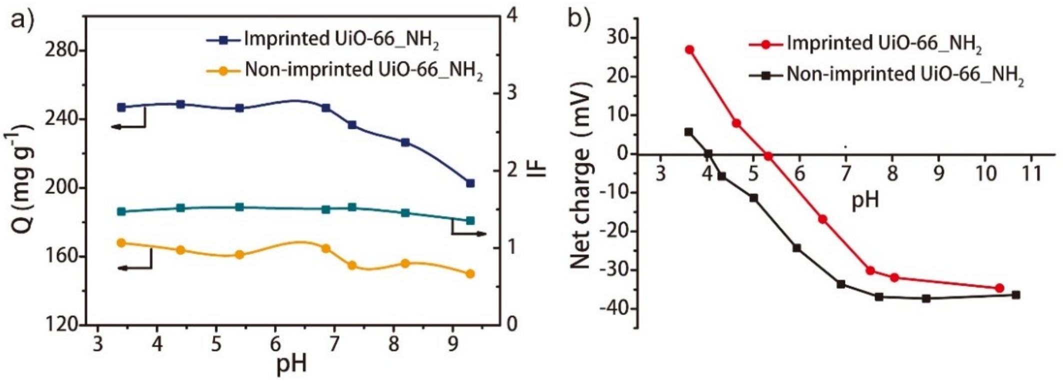

Fig. S2. (a) Effect of sample solution pH on the adsorption performance of KET over the imprinted UiO-66_NH_2 and non-imprinted UiO-66_NH_2, (b) zeta potentials of imprinted UiO-66_NH_2 and non-imprinted UiO-66_NH_2.

7. Adsorption isotherms and kinetics of KET on the imprinted UiO-66_NH_2

To investigate the specific binding capacity of KET on the imprinted UiO-66_NH_2 and non-imprinted UiO-66_NH_2, the adsorption isothermal experiments were tested by adding imprinted UiO-66_NH_2 or non-imprinted UiO-66_NH_2 (0.2 mg mL^{-1}) into KET aqueous solution (pH=6.8) with different concentrations ranging from 50 to 150 mg L^{-1}. After incubation of 90 min at room temperature, the solutions were isolated by centrifuging. The KET concentration in the supernatants was detected by HPLC to evaluate the specific adsorption capacity. All the experiments were conducted in triplicate. The equilibrium adsorption capacity (Q_e, mg g^{-1}) was calculated using the following equation:

$$Q_e = \frac{(C_0 - C_e)v}{m}$$

Where C_0 and C_e were the initial concentration of the template (KET) (mg L^{-1}) and the equilibrium concentration of the template (mg L^{-1}) in the supernatant after the adsorption, respectively. v was the volume of the sample solution (mL), and m was the mass of adsorbent (mg), respectively.

The specific recognition ability of KET on the imprinted UiO-66_NH_2 was evaluated by the imprinted factor (IF), which was defined as follows:

$$\text{Imprinted factor (IF)} = \frac{Q_{MIP}}{Q_{NIP}}$$

Where Q_{MIP} and Q_{NIP} were the equilibrium binding capacity of the template (KET) on the imprinted UiO-66_NH_2 and non-imprinted UiO-66_NH_2, respectively.

The adsorption kinetic experiments were conducted by incubating the imprinted UiO-66_NH_2 or non-imprinted UiO-66_NH_2 (0.2 mg mL^{-1}) with KET aqueous solution (pH=6.8, 50 mg L^{-1}). After incubation at different time intervals (2-90 min), the supernatants were collected for measurement.

To evaluate the selective recognition ability of KET on the imprinted UiO-66_NH_2, the selective adsorption experiments of imprinted UiO-66_NH_2 were first performed in the single system (containing only one substance in solution). Seven substances, including NAP, SDM, RhB, benzoic acid, CAF, PRO and phenol, were selected as the interferences of KET. Typically, 2 mg of imprinted UiO-66_NH$_2$ or non-imprinted UiO-66_NH$_2$ was added into 10 mL of aqueous solution (pH=6.8) containing only one substance with each concentration of 0.2 mmol L^{-1}. After incubation for 90 min, the supernatants were collected for measurement, and the substances in the supernatants were analyzed by HPLC or UV-vis spectrophotometer. Moreover, the competitive binding of KET on the imprinted UiO-66_NH$_2$ was studied in the binary systems containing KET and another interference (NAP, SDM RhB, benzoic acid and phenol). Here, 2 mg of imprinted UiO-66_NH$_2$ or non-imprinted UiO-66_NH$_2$ was added into 10 mL of binary mixture aqueous solutions (pH=6.8) with each substance concentration of 0.2 mmol L^{-1}. After incubation for 90 min, the supernatants were collected for measurement, and the mixed substances in the supernatants were analyzed by HPLC for the calculation of the displacement of KET.

The selective recognition ability of imprinted UiO-66_NH$_2$ was assessed by the selectivity factor (α), which was defined as follows:

$$\text{Selectivity factor } (\alpha) = \frac{IF_{tem}}{IF_{ana}}$$

Where IF_{tem} and IF_{ana} were the IF of the template (KET) and analogues (or interferents), respectively.

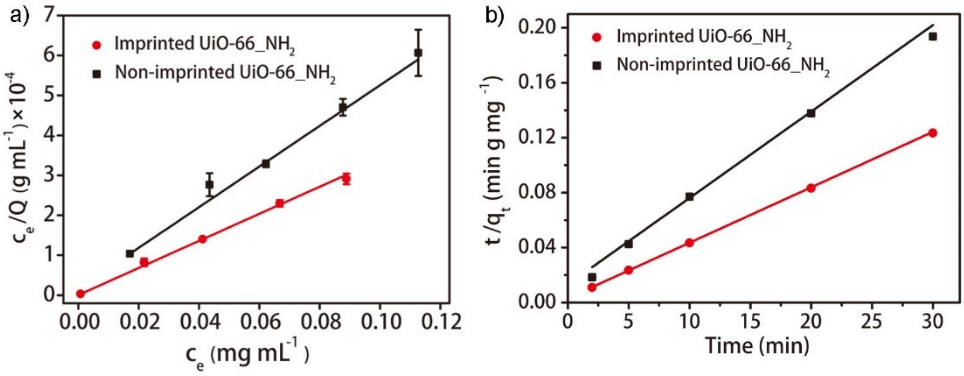

Fig. S3. (a) Theoretical Langmuir adsorption isotherms of KET on the imprinted UiO-66_NH$_2$ and non-imprinted UiO-66_NH$_2$, (b) pseudosecond-order model of adsorption dynamics of KET (50 mg L^{-1}) on the imprinted UiO-66_NH$_2$ and non-imprinted UiO-66_NH$_2$. Conditions: adsorbents (0.2 mg mL^{-1}), initial solution pH 6.8.

Table S2. Langmuir model parameters of binding capacity of KET on the imprinted UiO-66_NH$_2$ and non-imprinted UiO-66_NH$_2$.

Samples	**Model**	$q_{\max}$ **(mg g^{-1})**	K_L **(mL mg^{-1})**
Imprinted UiO-66_NH$_2$	Langmuir	295.2	7057.0
Non-imprinted UiO-66_NH$_2$		196.6	300.7

Table S3. Comparison of the templates (KET or SM2) sorption with different MIP adsorbents.

Adsorbents	**Template**	**Adsorption solvent**	$q_{\max}$ **(mg g^{-1})**	**Preparation method**	**Reference**
Silica@MIP microspheres	KET	Methanol/H$_2$O (10/90, v/v)	4.54	Surface imprinting polymerization	[1]
Silica@MIPs	SM2	Acetonitrile	33.87	Surface imprinting polymerization	[2]
Fe$_3$O$_4$@MIPs	SM2	Acetonitrile	0.68	Surface imprinting polymerization	[3]
MIP microspheres	SM2	Acetonitrile	47.46	Precipitation polymerization	[4]
MIPs	SMZ	H$_2$O	16.45	Bulk polymerization	[5]
Monolithic MIPs	SMZ	Acetonitrile/H$_2$O (30/70, v/v)	30.89	Bulk polymerization	[6]
Imprinted MIL-101_NH$_2$	SM2	Methanol/H$_2$O (5/95, v/v)	192.3	In-situ self-assembly polymerization	This work
Imprinted UiO-66_NH$_2$	KET	H$_2$O	295.2	In-situ self-assembly polymerization	This work

Table S4. Pseudosecond-order model parameters of the binding kinetics of KET on the imprinted UiO-66_NH$_2$ and non-imprinted UiO-66_NH$_2$.

Samples	**R^2 value**	q_e **(mg g^{-1})**	$K_2q_e^2$ **(mg g^{-1} min^{-1})**
Imprinted UiO-66_NH$_2$	0.98	247.5	312.5
Non-imprinted UiO-66_NH$_2$	0.98	159.0	75.8

Table S5. Imprinting factor (IF) and selectivity factor (α) of the imprinted UiO-66_NH$_2$.

Substances	Q_{MIP} **(mg g^{-1})**	Q_{NIP} **(mg g^{-1})**	**IF$_{(Q\mathrm{MIP}/Q\mathrm{NIP})}$**	α
KET	250.5	163.6	1.5	-
NAP	219.4	165.1	1.3	1.2
SDM	187.0	178.3	1.0	1.5
RhB	36.4	18.9	1.9	0.8
Benzoic acid	38.2	41.9	0.9	1.7
CAF	18.1	19.2	0.9	1.7

PRO	3.8	2.3	1.7	0.9
Phenol	0.9	0.6	1.5	1.0

8. Universality of the molecular imprinting approach

8.1 Synthesis of sulfadimidine (SM2) imprinted MIL-101_NH_2

SM2 imprinted MIL-101_NH_2 was synthesized by the same method as KET imprinted UiO-66_NH_2. Briefly, 0.675 g of $FeCl_3 \cdot 6H_2O$ and 0.346 g of SM2 were mixed in 15 mL of DMF. The mixture was stirred for 10 min to obtain a clear solution, and then 0.225 g of NH_2-BDC was added. After stirring for another 10 min, the dissolved reaction mixture was transferred into a 25 mL Teflon liner. The Teflon liner was sealed and placed in a preheated oven at 110 ℃ for 24 h. After cooling to room temperature, the product was isolated by centrifuging at 10000 rpm for 10 min. The product was washed with ethanol at 60 ℃ for 3 h. The washing step was repeated 2-3 times until no SM2 template was detected by HPLC in the supernatant. The powder was separated and dried in vacuum oven at 100 ℃ for 12 h. In this way, the imprinted MIL-101_NH_2 was obtained. The non-imprinted MIL-101_NH_2 was prepared in the same way as that for the imprinted MIL-101_NH_2 except the addition of the SM2 template.

8.2 Adsorption performance of SM2 on the imprinted MIL-101_NH_2

To improve the solubility of SM2 in aqueous solution (pH was not adjusted), an appropriate ratio of methanol should be added. The effect of methanol content on the adsorption performance of SM2 over the imprinted MIL-101_NH_2 and non-imprinted MIL-101_NH_2 was investigated. As shown in **Fig. S4**, the adsorption capacities of SM2 on both imprinted MIL-101_NH_2 and non-imprinted MIL-101_NH_2 decreased rapidly with the increase of methanol content in adsorption solution, which was due to the competition binding of methanol (with the template SM2) on the active sites inside MOFs. The IF of imprinted MIL-101_NH_2 showed the highest value when the content of methanol added in aqueous solution was 5 vol%. Therefore, a mixture solution of water and methanol (95/5, v/v) was selected as the optimized solution for the following adsorption experiments.

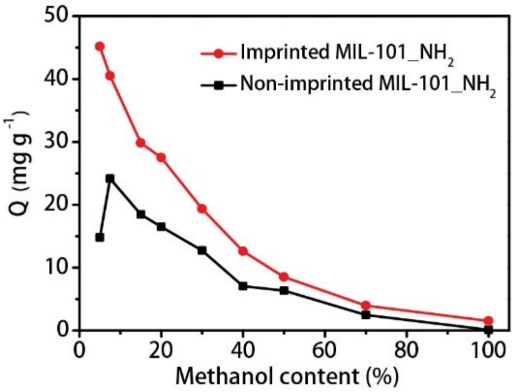

Fig. S4. Effect of methanol content on adsorption performance of SM2 over the imprinted MIL-101_NH$_2$ and non-imprinted MIL-101_NH$_2$. Conditions: adsorbents (5 mg mL^{-1}), SM2 (400 mg L^{-1}), initial solution pH (not adjusted).

The specific binding capacity of SM2 on the imprinted MIL-101_NH$_2$ and non-imprinted MIL-101_NH$_2$ were also determined. Typically, 5 mg of imprinted MIL-101_NH$_2$ or non-imprinted MIL-101_NH$_2$ was added into 1 mL of SM2 solution [a mixture of water and methanol (95/5, v/v)] with various concentration of SM2 ranging from 25 to 400 mg L^{-1}. After incubation of 120 min at room temperature, the solutions were isolated by centrifuging, and the concentration of SM2 in the supernatants was determined by HPLC analysis. All the experiments were conducted in triplicate.

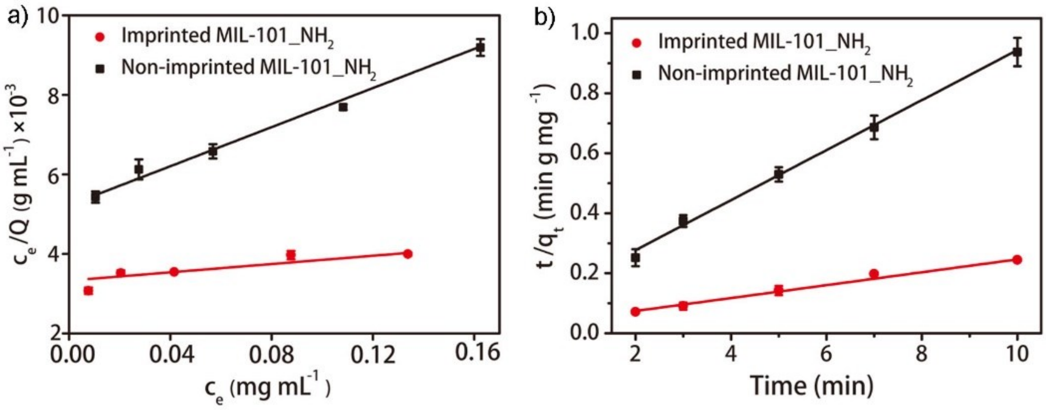

Fig. S5. (a) Theoretical Langmuir adsorption isotherms of SM2 on the imprinted MIL-101_NH$_2$ and non-imprinted MIL-101_NH$_2$, (b) pseudosecond-order model of adsorption dynamics of SM2 (400 mg L^{-1}) on the imprinted MIL-101_NH$_2$ and non-imprinted MIL-101_NH$_2$. Conditions: adsorbents (5 mg mL^{-1}), adsorption solution (5% methanol and 95% water, v/v), adsorption solution pH (not adjusted).

Table S6. Langmuir model parameters of binding capacity of SM2 on the imprinted MIL-101_NH$_2$ and non-imprinted MIL-101_NH$_2$.

Samples	**Model**	**$q_{\max}$ (mg g^{-1})**	**K_L (mL mg^{-1})**

Imprinted MIL-101_NH$_2$	Langmuir	192.3	1.6
Non-imprinted MIL-101_NH$_2$		40.7	4.7

Table S7. Pseudosecond-order model parameters of binding kinetics of SM2 on the imprinted MIL-101_NH$_2$ and non-imprinted MIL-101_NH$_2$.

Samples	**R^2 value**	**q_e (mg g^{-1})**	**$K_2q_e^2$ (mg g^{-1} min^{-1})**
Imprinted MIL-101_NH$_2$	0.98	46.5	31.8
Non-imprinted MIL-101_NH$_2$	0.98	12.0	9.1

8.3 Binding selectivity of SM2 on the imprinted MIL-101_NH$_2$

To evaluate the selectivity of SM2 on the imprinted MIL-101_NH$_2$, four compounds, including SMZ, SB, MA and SA, were selected as the analogues of SM2. Typically, 5 mg of imprinted MIL-101_NH$_2$ or non-imprinted MIL-101_NH$_2$ was dispersed into 1 mL of a mixture of water and methanol (95/5, v/v) containing only one substance with each concentration of 400 mg L^{-1}. The adsorption solutions were incubated at room temperature for 120 min, and then the supernatants were collected for the measurement of the compound concentration. The IF and α of the imprinted MIL-101_NH$_2$ were summarized in **Table S8**.

Table S8. The IF and α of the imprinted MIL-101_NH$_2$.

Substances	**Q_{MIP} (mg g^{-1})**	**Q_{NIP} (mg g^{-1})**	**IF$_{(Q\text{MIP}/Q\text{NIP})}$**	**α**
SM2	45.2	14.8	3.1	-
SMZ	31.7	23.6	1.3	2.3
SB	62.1	29.3	2.1	1.4
MA	10.0	5.3	1.9	1.6
SA	4.6	4.4	1.0	2.9

9. Photocatalytic degradation of SM2 on the imprinted MIL-101_NH$_2$ and non-imprinted MIL-101_NH$_2$

The photocatalytic degradation experiments in the presence of H_2O_2 were performed in a cylindrical glass reactor with a diameter of 9 cm. A 100W LED visible light lamp (λ_{max}=445 nm) as the light source was located in the axial position. Typically, 25 mg of imprinted MIL-101_NH$_2$ was immersed into 50 mL of SM2 aqueous solution (pH=4) with the concentration of 20 mg L^{-1}, and the dispersion solution was stirred in the dark for 60 min to achieve the adsorption/desorption equilibrium. Subsequently, the photocatalytic degradation of SM2 was started after the irradiation of the LED lamp and the addition of 10 mmol L^{-1} of H_2O_2. Aliquots (1 mL) of the solution were sampled at different time intervals, and immediately filtered through a 0.22 μm membrane for the measurement of the concentration of SM2 by HPLC.

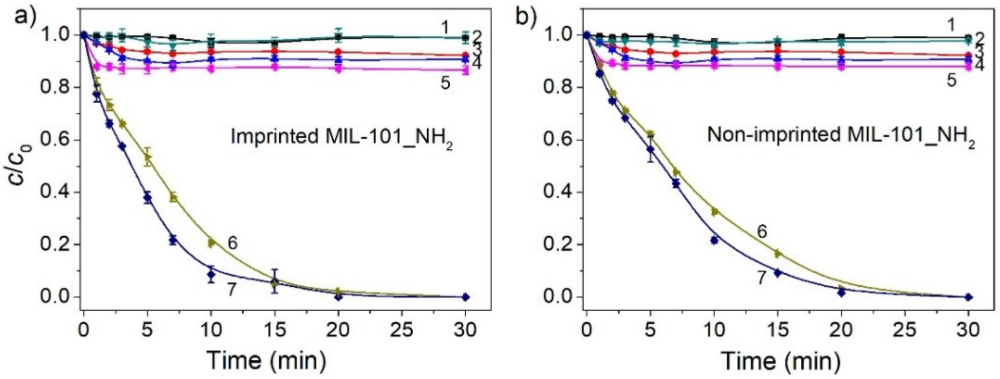

Fig. S6. Degradation of SM2 on the imprinted MIL-101_NH$_2$ (a) and non-imprinted MIL-101_NH$_2$ (b). Various conditions: (1) visible light; (2) catalyst and visible light; (3) H_2O_2; (4) H_2O_2 and visible light; (5) catalyst; (6) catalyst and H_2O_2; (7) catalyst, H_2O_2 and visible light. Reaction conditions: SM2 (20 mg L^{-1}), catalyst (0.5 mg mL^{-1}), H_2O_2 (10 mmol L^{-1}), initial aqueous solution pH 4.0.

10. Selective photocatalytic degradation of SM2 on the imprinted MIL-101_NH$_2$

The selective degradation experiments of SM2 on the imprinted MIL-101_NH$_2$ in the binary system containing SM2 and another analogue were carried out. Four substances, including SMZ, SMM, SB and 4NP, were selected as the analogues of SM2. Here, 25 mg of imprinted MIL-101_NH$_2$ was immersed into 50 mL of aqueous solution (pH=4) containing binary substances with the concentration of 2 mg L^{-1} for SM2 and 40 mg L^{-1} for another analogue. After adsorption/desorption equilibrium, the photocatalytic degradation was started after the irradiation of the LED lamp and the addition of 10 mmol L^{-1} of H_2O_2. Aliquots (1 mL) of the solution were sampled at different time intervals, and immediately filtered through a 0.22 μm membrane for analysis of SM2 and coexisted analogue by HPLC. The rate constant (*k*) values of SM2 on the imprinted MIL-101_NH$_2$ in the absence and presence of high level analogues were illustrated in **Fig. S7**.

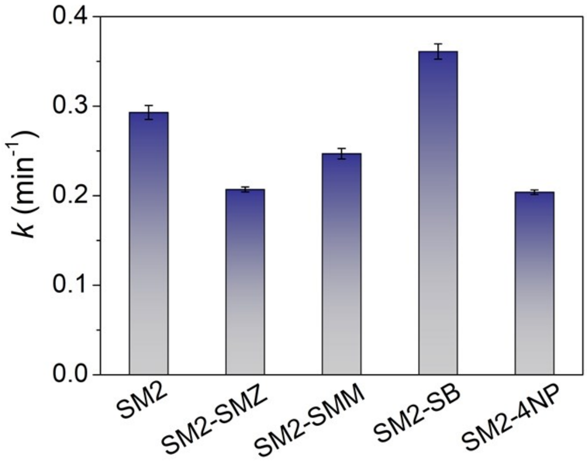

Fig. S7. Rate constant (*k*) values for the photocatalytic degradation of the template SM2 on the imprinted MIL-101_NH$_2$ in the single system (SM2) and binary systems (SM2-SMZ, SM2-SMM, SM2-SB and SM2-4NP). Conditions: catalyst (0.5 mg mL^{-1}), H$_2$O$_2$ (10 mmol L^{-1}), SM2 (2 mg L^{-1}), analogues (SMZ, SMM, SB and 4NP) (40 mg L^{-1}), initial aqueous solution pH 4.0.

Reference

[1] J. Jiang, K. Song, Z. Chen, Q. Zhou, Y. Tang, F. Gu, X. Zuo, Z. Xu, *J. Chromatogr. A*, 2011, **1218**, 3763-3770.

[2] Y. Li, X. Li, Y. Li, C. Dong, P. Jin, J. Qi, *Biomaterials*, 2009, **30**, 3205-3211.

[3] X. Mao, H. Sun, X. He, L. Chen, Y. Zhang, *Anal. Methods*, 2015, **7**, 4708-4716.

[4] D. Peng, Z. Li, Y. Wang, Z. Liu, F. Sheng, Z. Yuan, *J. Chromatogr. A*, 2017, **1506**, 9-17.

[5] M. Valtchev, B.S. Palm, M. Schiller, U. Steinfeld, *J. Hazard. Mater.*, 2009, **170**, 722-728.

[6] X. Liu, C. Ouyang, R. Zhao, D. Shangguan, Y. Chen, G. Liu, *Anal. Chim. Acta*, 2006, **571**, 235-241.